Electronic Supplementary Material (ESI) for Journal of Materials Chemistry A.
This journal is © The Royal Society of Chemistry 2019

Supplementary Information

Cu:NiO as a hole-selective back contact to improve the photoelectrochemical performance of $CuBi_2O_4$ thin film photocathodes

Angang Song,[ab] Paul Plate,[a] Abdelkrim Chemseddine,[a] Fuxian Wang,[a] Fatwa F. Abdi,[a] Markus Wollgarten,[c] Roel van de Krol,[ab] and Sean P. Berglund[a*]
[a.] Institute for Solar Fuels, Helmholtz-Zentrum Berlin für Materialien und Energie GmbH, Institute for Solar Fuels, Hahn-Meitner-Platz 1, 14109 Berlin, Germany.
[b.] Institute für Chemie, Technische Universität Berlin, Straße des 17. Juni 124, 10623 Berlin, Germany
[c.] Department Nanoscale Structures and Microscopic Analysis, Helmholtz-Zentrum Berlin für Materialien und Energie GmbH, Hahn-Meitner-Platz 1, 14109 Berlin, Germany
* E-mail: sean.berglund@helmholtz-berlin.de

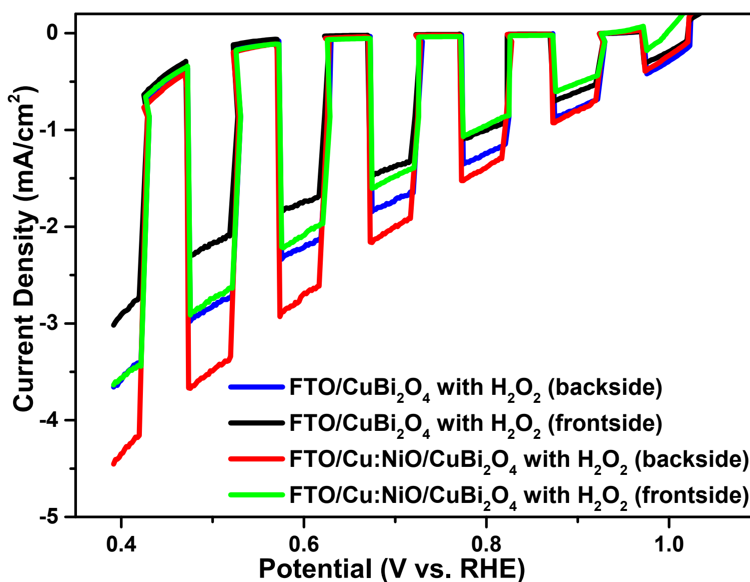

Figure S1. LSV scans for $CuBi_2O_4$ films on FTO and FTO/Cu:NiO (7 nm) at a thicknesses of 260 nm measured in 0.3 M K_2SO_4 and 0.2 M phosphate buffer (pH 6.65) with H_2O_2 added as an electron scavenger under backside and frontside illumination.

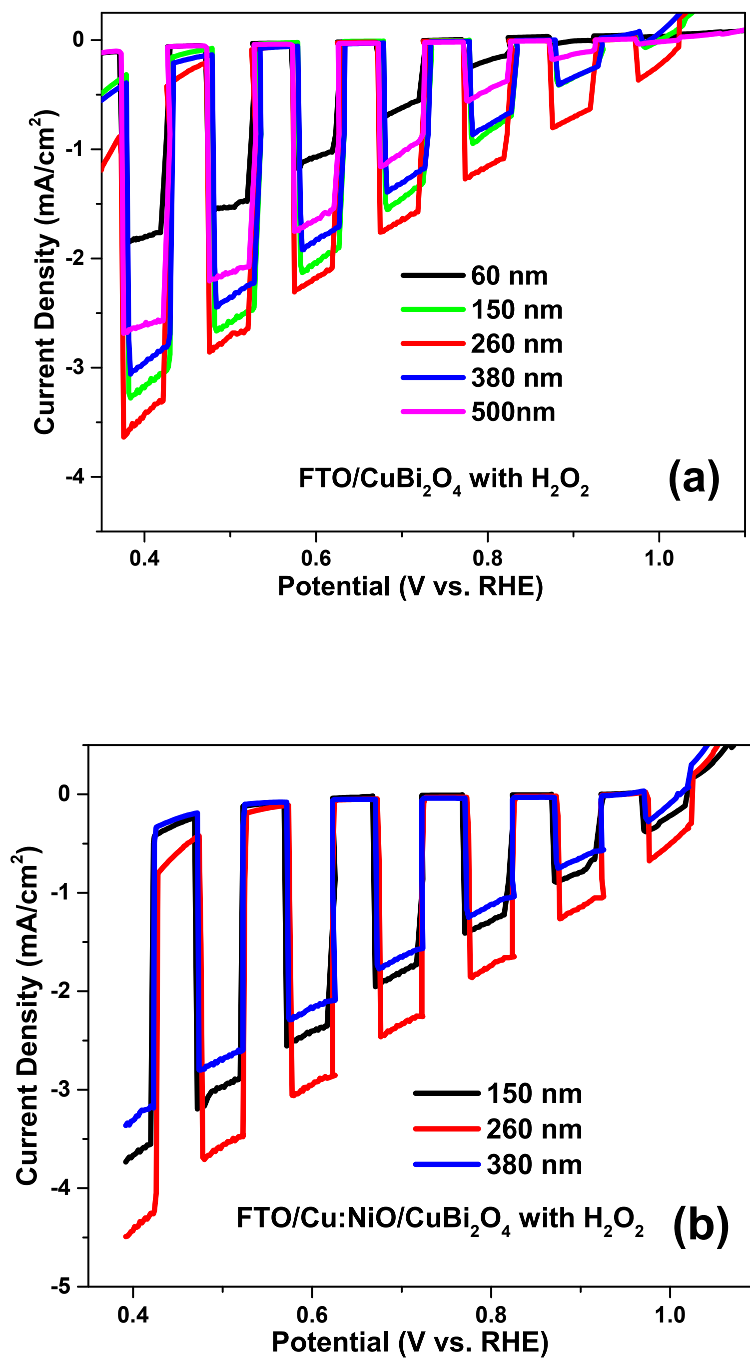

Figure S2. (a) LSV scans for FTO/$CuBi_2O_4$ and (b) FTO/Cu:NiO (7 nm)/$CuBi_2O_4$ films at different film thicknesses measured in 0.3 M K_2SO_4 and 0.2 M phosphate buffer (pH 6.65) with H_2O_2 added as an electron scavenger under backside illumination.

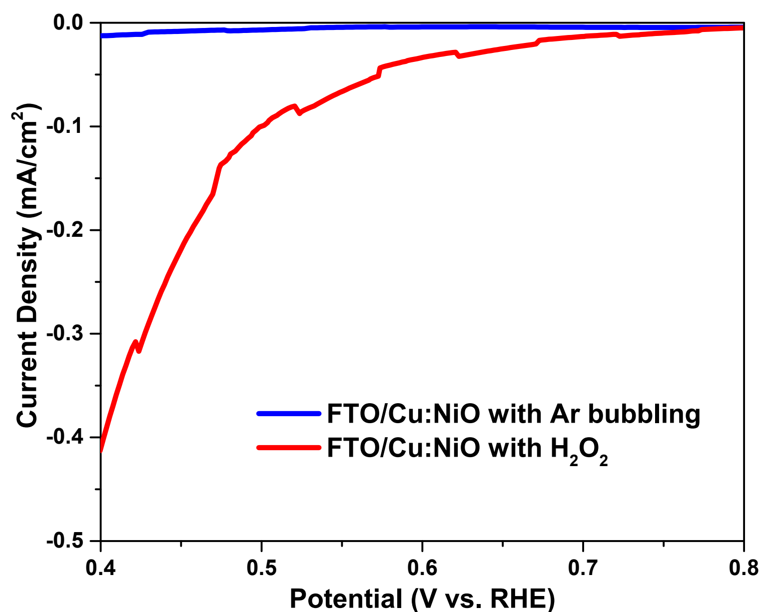

Figure S3. LSV scans for Cu:NiO at a thicknesses of 34 nm measured in 0.3 M K_2SO_4 and 0.2 M phosphate buffer (pH 6.65) with Ar bubbling and with H_2O_2 under backside illumination.

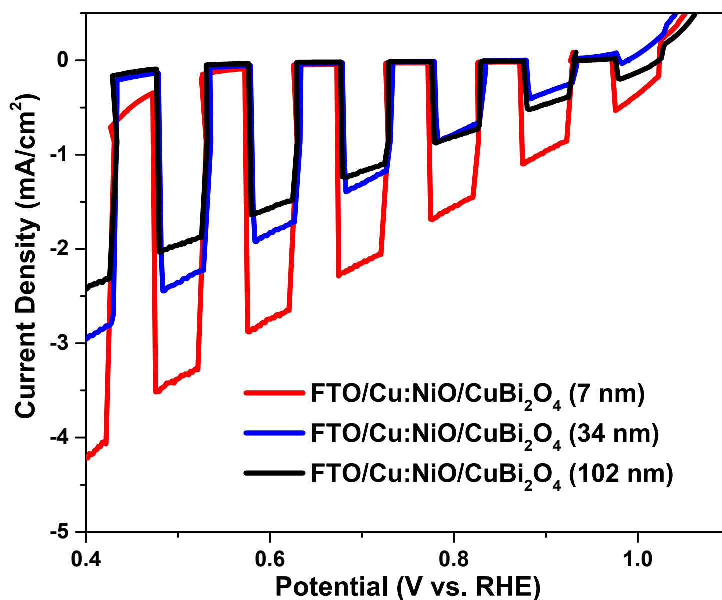

Figure S4. LSV scans for $CuBi_2O_4$ films (~260 nm) based on different film thicknesses of Cu:NiO (7, 34, and 102 nm) measured in 0.3 M K_2SO_4 and 0.2 M phosphate buffer (pH 6.65) with H_2O_2 under backside illumination.

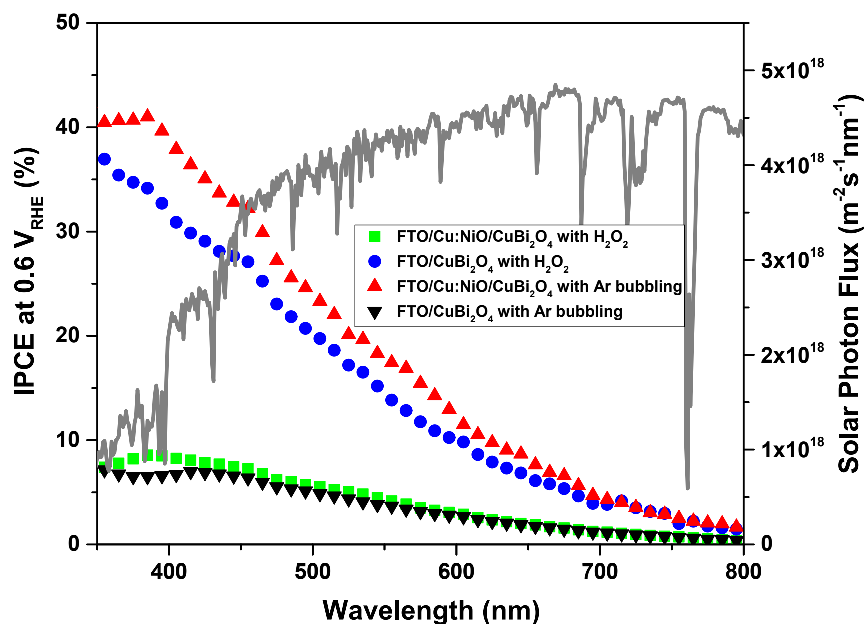

Figure S5. IPCE spectra of $CuBi_2O_4$ on FTO (blue dot line), $CuBi_2O_4$ on Cu:NiO (red and green dot line). The measurements were performed in 0.3 M K_2SO_4 and 0.2 M phosphate buffer (pH 6.65) with H_2O_2 under backside illumination.

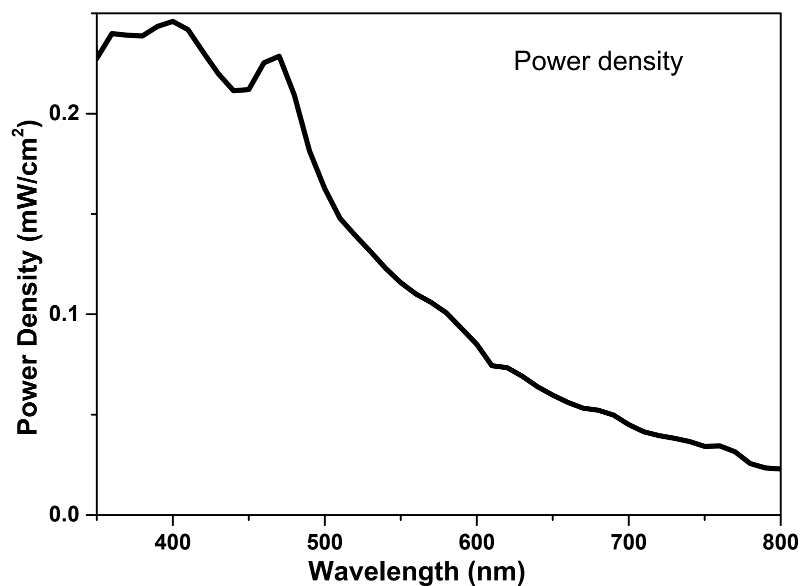

Figure S6. Power spectra for back illumination IPCE measurements.

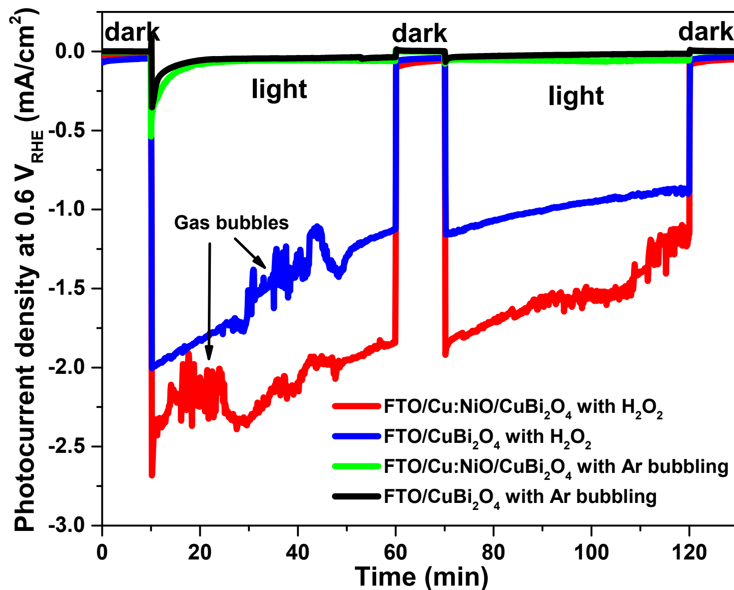

Figure S7. Constant potential measurement at 0.6 V vs RHE for 260 nm $CuBi_2O_4$ films based on bare FTO and 7 nm Cu:NiO in the dark and light (AM1.5 irradiation). Measurements were done in 0.3 M K_2SO_4 and 0.2 M phosphate buffer (pH 6.65) with Ar bubbling and with H_2O_2 under backside illumination.

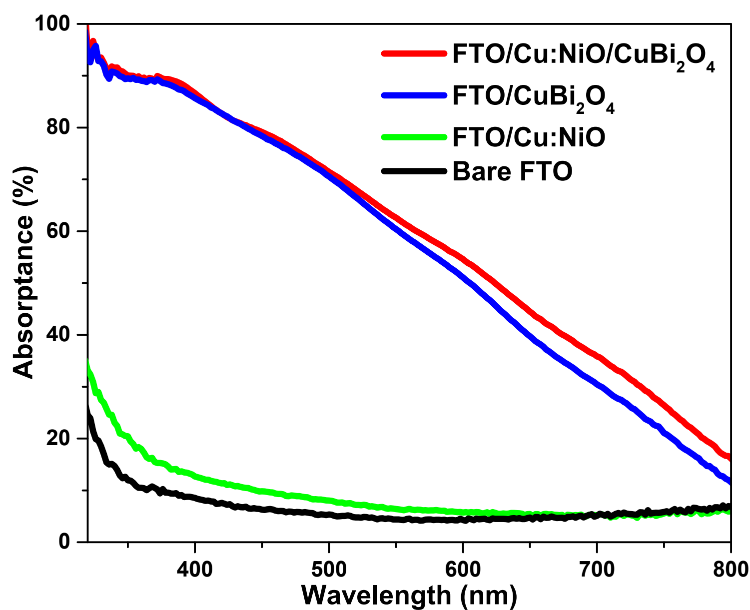

Figure S8. Absorptance spectra for bare FTO, FTO/Cu:NiO (7nm) and FTO/$CuBi_2O_4$ and FTO/Cu:NiO (7nm)/$CuBi_2O_4$.

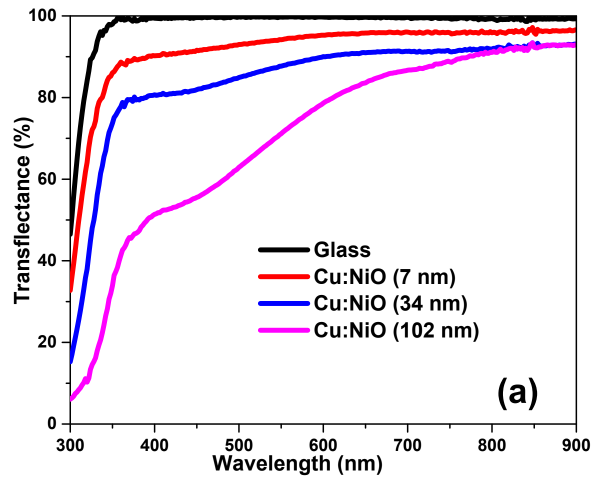

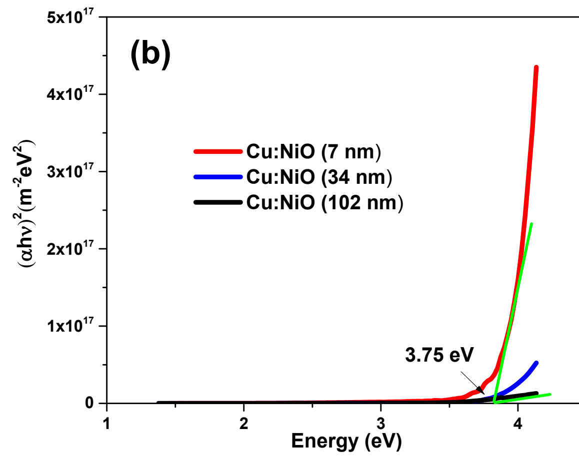

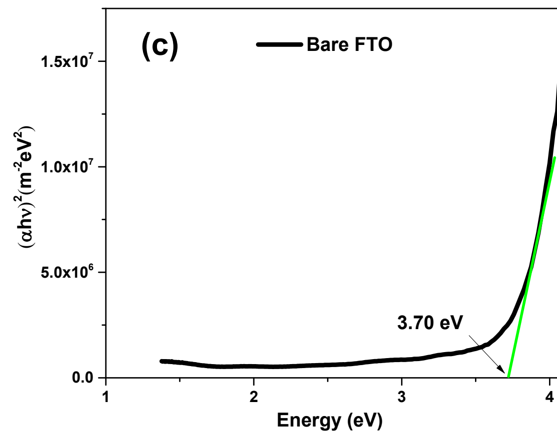

Figure S9. (a) Transflectance spectra and (b) direct bandgap Tauc plots for Cu:NiO thin films with different thicknesses (7, 34, and 102 nm) deposited on glass substrates and (c) direct band gap Tauc plot of FTO substrate.

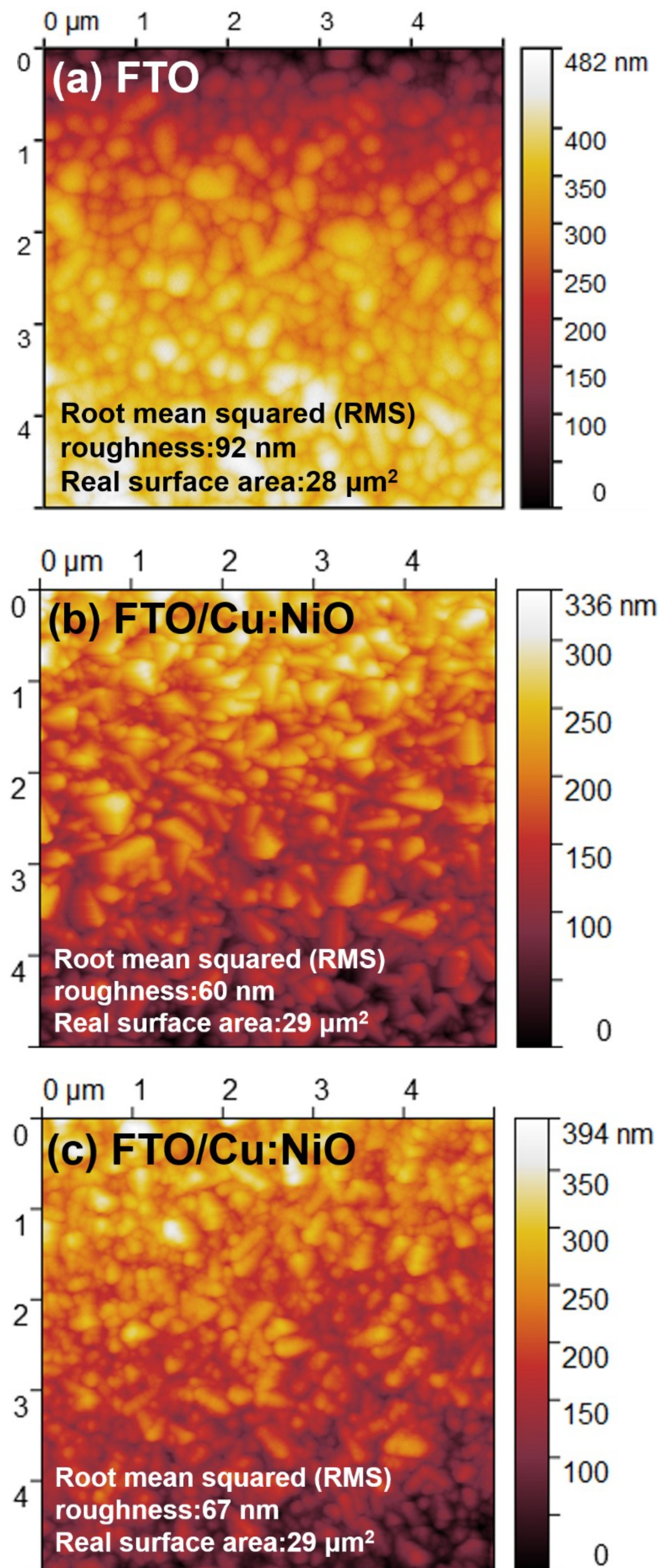

Figure S10. AFM images of (a) bare FTO, and (b) a 7 nm Cu:NiO layer, and (c) a 34 nm Cu:NiO layer deposited on FTO

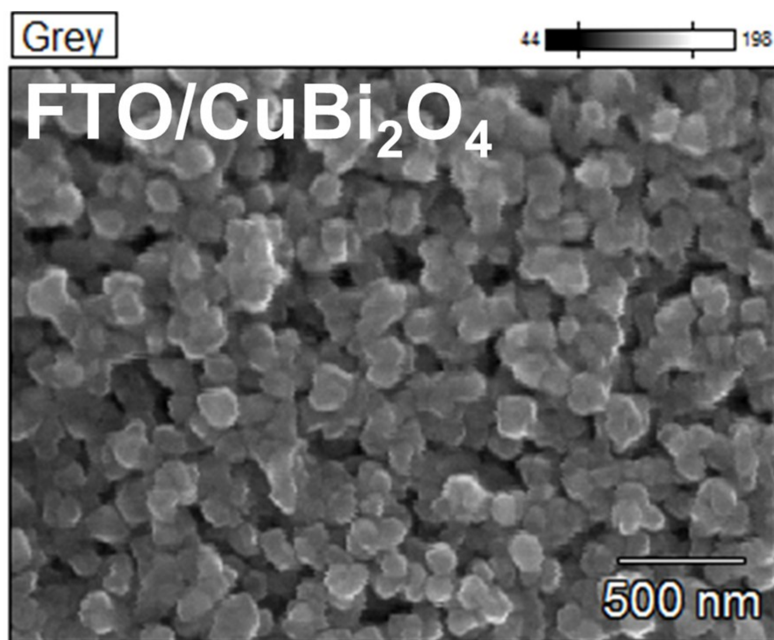

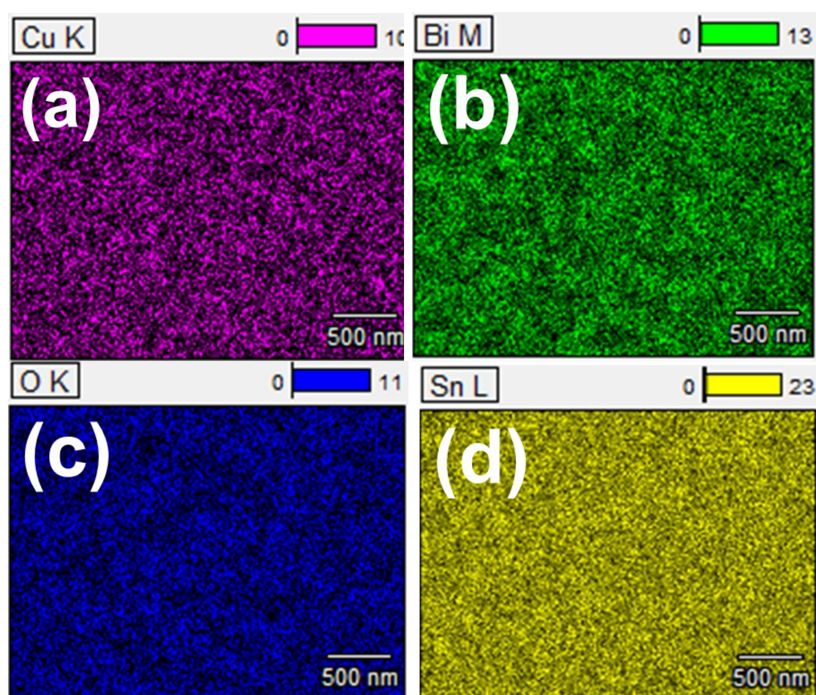

Figure S11. Top-view SEM image of 260 nm $CuBi_2O_4$ deposited on FTO and corresponding EDX elemental mapping of (b) Cu (c) Bi, (d) O and (d) Sn.

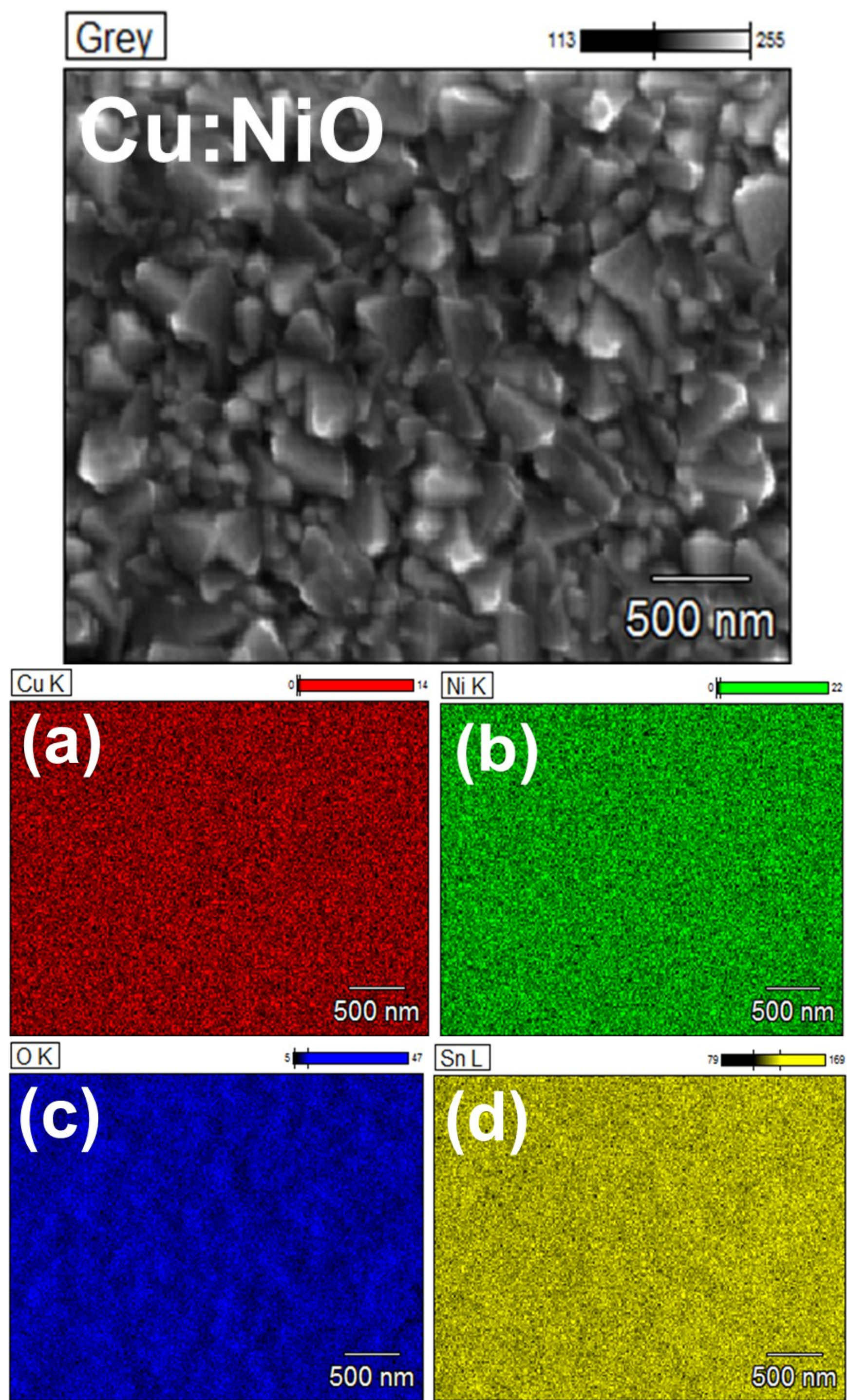

Figure S12. Top-view SEM image of 7 nm Cu:NiO thin film deposited on FTO and corresponding EDX elemental mapping of (b) Cu (c) Bi, (d) O, and (e) Sn.

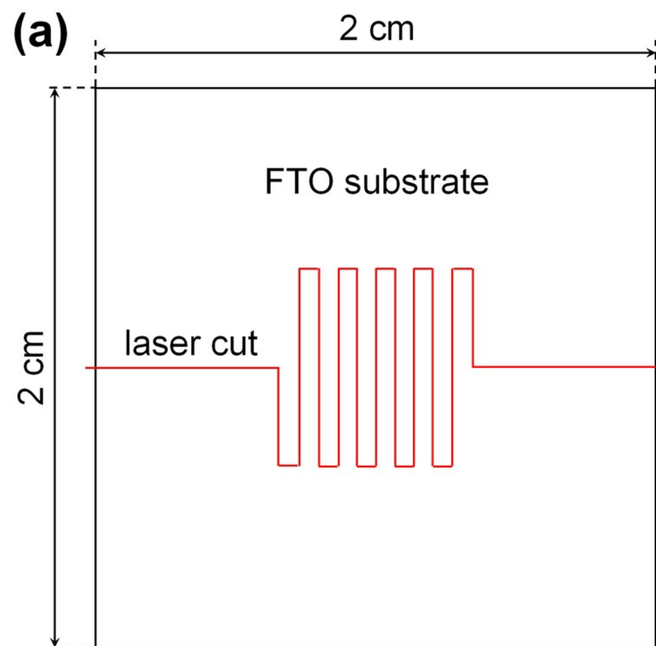

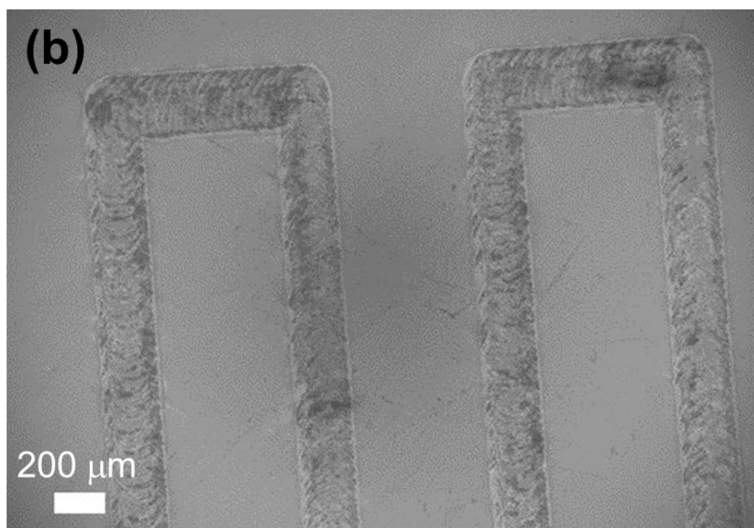

Figure S13. (a) Drawing of the laser cut pattern used for solid-state I-V measurements. (b) SEM image of an FTO substrate with a laser cut.

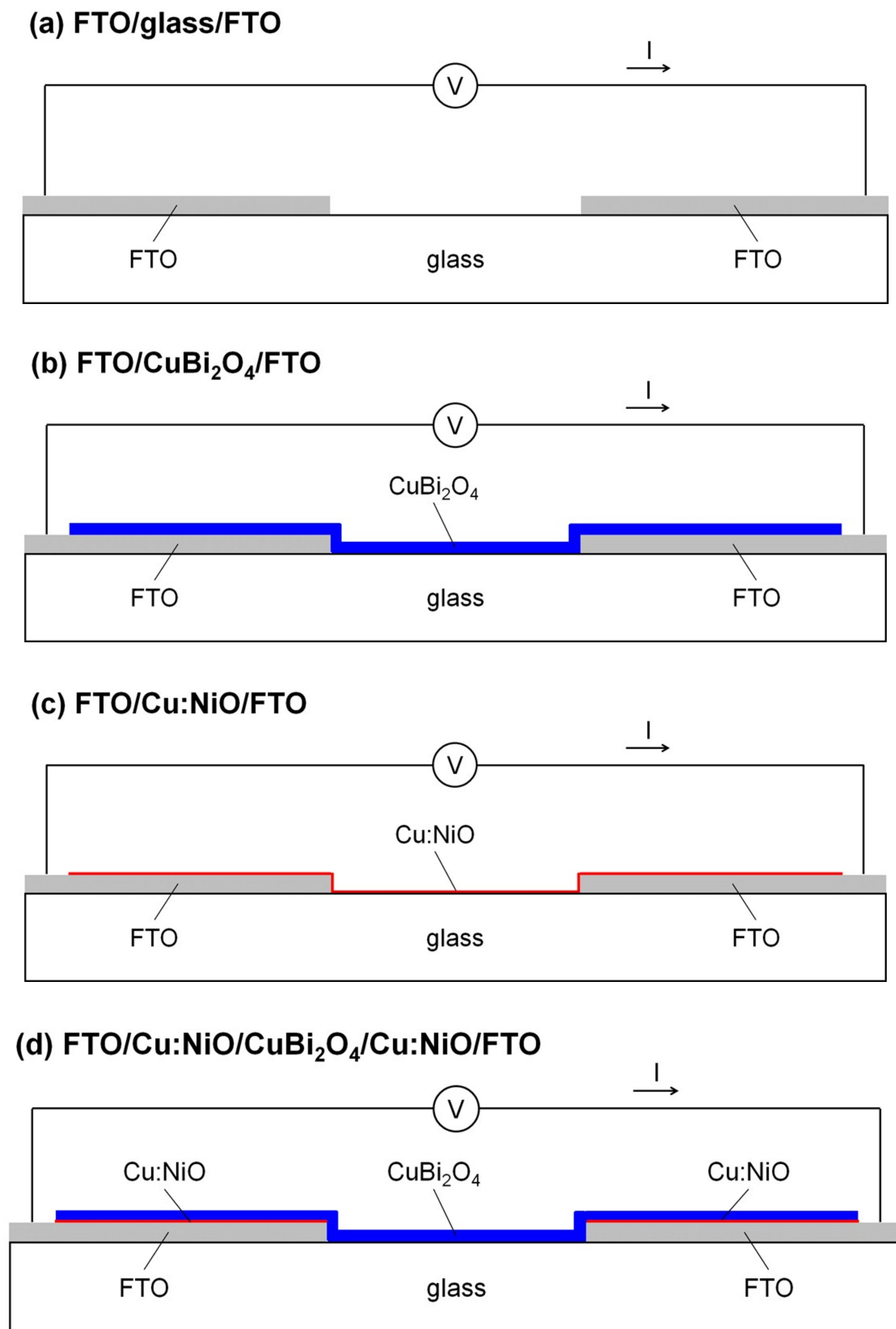

Figure S14. Schematics of the (a) FTO/glass/FTO, (b) FTO/$CuBi_2O_4$/FTO, (c) FTO/Cu:NiO/FTO, and (d) FTO/Cu:NiO/$CuBi_2O_4$/Cu:NiO/FTO samples used for solid-state I-V measurements. The $CuBi_2O_4$ and Cu:NiO thicknesses were 260 and 7 nm, respectively.

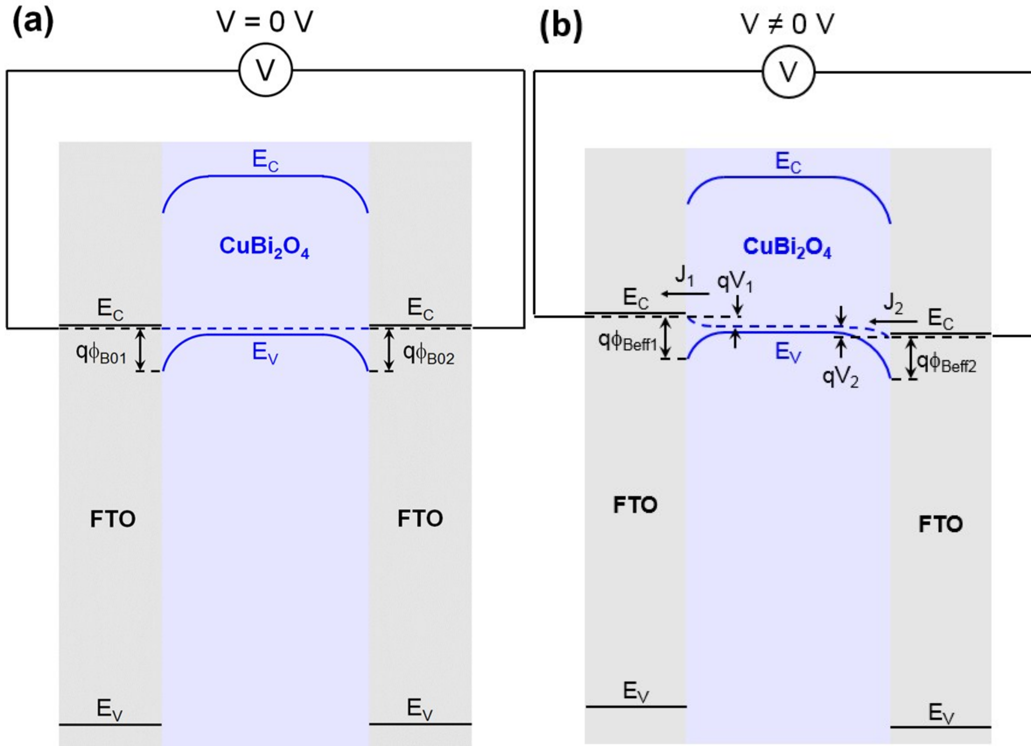

Figure S15. Schematic illustrating the band bending of back-to-back Schottky barriers (FTO/$CuBi_2O_4$/FTO sample) at (a) V = 0 V and (b) V ≠ 0 V.

Derivation of Equation for Back-to-Back Schottky Diodes

The current densities across back-to-back Schottky barriers, J_1 and J_2 (A/cm^2), are governed by the following equations.[1-5]

$$J_1 = A^{**}\, T^2 \exp\left(\frac{-\,q\phi_{Beff1}}{kT}\right)\left[\exp\left(\frac{qV}{kT}\right) - 1\right]$$

$$J_1 = J_{s1}\left[\exp\left(\frac{qV}{kT}\right) - 1\right]$$

$$J_2 = -A^{**}\, T^2 \exp\left(\frac{-\,q\phi_{Beff2}}{kT}\right)\left[\exp\left(\frac{qV}{kT}\right) - 1\right]$$

$$J_2 = -J_{s2}\left[\exp\left(\frac{-\,qV}{kT}\right) - 1\right]$$

A** is the reduced effective Richardson Constant (A cm^{-2} K^{-2}), T is the temperature (K), q is the electronic charge (1.602 × 10^{-19} C), k is the Boltzmann constant (1.381 × 10^{-23} m^2 kg s^{-2} K^{-1}), ϕ_{Beff1} and ϕ_{Beff2} are the effective barrier heights (eV), V is the overall applied voltage (V), and V_1 and V_2 are resulting voltages at each back-to-back Schottky barrier (V).

From continuity and symmetry, the overall current density (J) and applied voltage (V) are related to the individual values as follows:

$J = J_1 = J_2$

$$V = V_1 + V_2$$

Substitution of variables can be used to solve for J.

$$V_1 = \frac{kT}{q} \ln \left[1 + \frac{J}{J_{s1}}\right]$$

$$V_2 = \frac{-kT}{q} \ln \left[1 - \frac{J}{J_{s2}}\right]$$

$$V = \frac{kT}{q} \ln \left[1 + \frac{J}{J_{s1}}\right] - \frac{kT}{q} \ln \left[1 - \frac{J}{J_{s2}}\right]$$

$$J = \frac{J_{s1} J_{s2} \exp\left(\frac{qV}{2kT}\right) - J_{s1} J_{s2} \exp\left(\frac{-qV}{2kT}\right)}{J_{s1} \exp\left(\frac{qV}{2kT}\right) + J_{s2} \exp\left(\frac{-qV}{2kT}\right)}$$

$$J = \frac{J_{s1} J_{s2} \sinh\left(\frac{qV}{2kT}\right)}{J_{s1} \exp\left(\frac{qV}{2kT}\right) + J_{s2} \exp\left(\frac{-qV}{2kT}\right)}$$

Under the assumption that the barrier height of each Schottky barrier, scales linearly with the applied voltage, the effective barrier heights can be defined in terms of the ideality factors, n_1 and n_2.

$$\phi_{Beff1} = \phi_{B01} + V_1\left(1 - \frac{1}{n_1}\right)$$

$$\phi_{Beff2} = \phi_{B02} - V_2\left(1 - \frac{1}{n_2}\right)$$

ϕ_{B01} and ϕ_{B02} are the barrier heights at zero bias (eV).

$$J = \frac{2\,A^{**}\,T^2 \exp\left(\frac{-q\left[\phi_{B01} + V_1\left(1-\frac{1}{n_1}\right)\right]}{kT}\right) A^{**}\,T^2 \exp\left(\frac{-q\left[\phi_{B02} - V_2\left(1-\frac{1}{n_2}\right)\right]}{kT}\right) \sinh\left(\frac{qV}{2kT}\right)}{A^{**}\,T^2 \exp\left(\frac{-q\left[\phi_{B01} + V_1\left(1-\frac{1}{n_1}\right)\right]}{kT}\right) \exp\left(\frac{qV}{2kT}\right) + A^{**}\,T^2 \exp\left(\frac{-q\left[\phi_{B02} - V_2\left(1-\frac{1}{n_2}\right)\right]}{kT}\right) \exp\left(\frac{-qV}{2kT}\right)}$$

By the symmetry of the system the back-to-back Schottky diodes should have similar barrier heights at zero bias and ideality factors.

$\phi_{B01} = \phi_{B02} = \phi_{B0}$

$n_1 = n_2 = n$

Furthermore, if the channel resistance is low, then voltages at each Schottky barrier can be assumed to be equal.

$$V_1 = V_2 = \frac{V}{2}$$

$$J = \frac{2\,A^{**}\,T^2 \exp\left(\frac{-2q\phi_{B0}}{kT}\right) \exp\left(\frac{-q(V-V)}{2kT}\right) \exp\left(\frac{-q(V-V)}{2nkT}\right) \sinh\left(\frac{qV}{2kT}\right)}{\exp\left(\frac{-q\phi_{B0}}{kT}\right)\left[\exp\left(\frac{-qV}{2kT}\right)\exp\left(\frac{qV}{2nkT}\right)\exp\left(\frac{qV}{2kT}\right) + \exp\left(\frac{-qV}{2kT}\right)\exp\left(\frac{-qV}{2nkT}\right)\exp\left(\frac{qV}{2kT}\right)\right]}$$

$$J = \frac{2\,A^{**}\,T^2 \exp\left(\frac{-2q\phi_{B0}}{kT}\right) \sinh\left(\frac{qV}{2kT}\right)}{\exp\left(\frac{qV}{2nkT}\right) + \exp\left(\frac{-qV}{2nkT}\right)}$$

$$J = \frac{A^{**}\,T^2 \exp\left(\frac{-2q\phi_{B0}}{kT}\right) \sinh\left(\frac{qV}{2kT}\right)}{\cosh\left(\frac{qV}{2nkT}\right)}$$

References

1. E. H. Rhoderick, *IEE Proceedings I - Solid-State and Electron Devices*, 1982, **129**, 1.
2. S. Sze, *Physics of semiconductor devices*, 2007, **3**.

3. X.-L. Tang, H.-W. Zhang, H. Su and Z.-Y. Zhong, *Physica E: Low-dimensional Systems and Nanostructures*, 2006, **31**, 103-106.
4. T. Nagano, M. Tsutsui, R. Nouchi, N. Kawasaki, Y. Ohta, Y. Kubozono, N. Takahashi and A. Fujiwara, *The Journal of Physical Chemistry C*, 2007, **111**, 7211-7217.
5. R. Nouchi, *Journal of Applied Physics*, 2014, **116**, 184505.

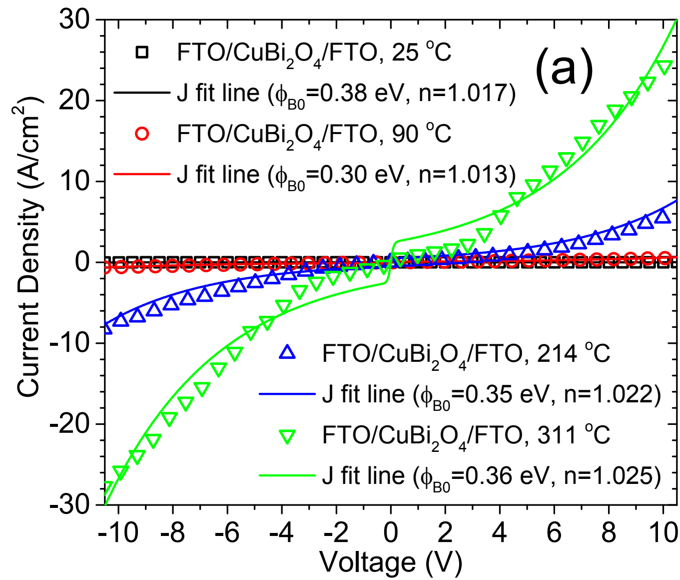

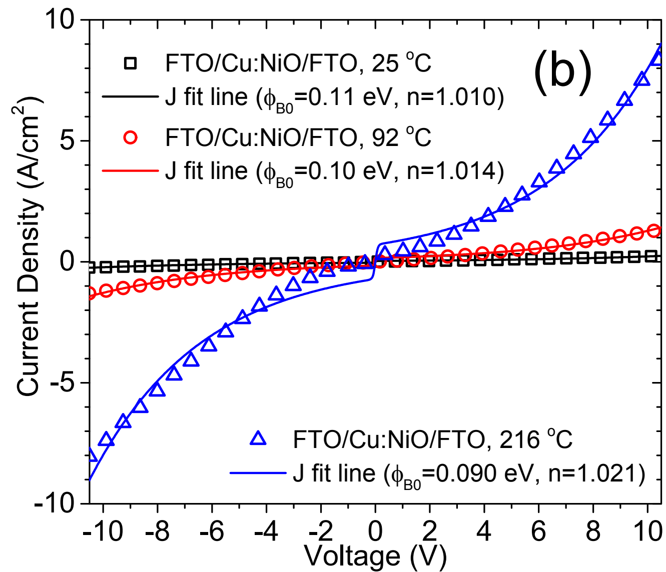

Figure S16. Current density vs. voltage (J-V) measurements at different temperatures for (a) FTO/$CuBi_2O_4$/FTO and (b) FTO/Cu:NiO/FTO samples with J fit lines included.

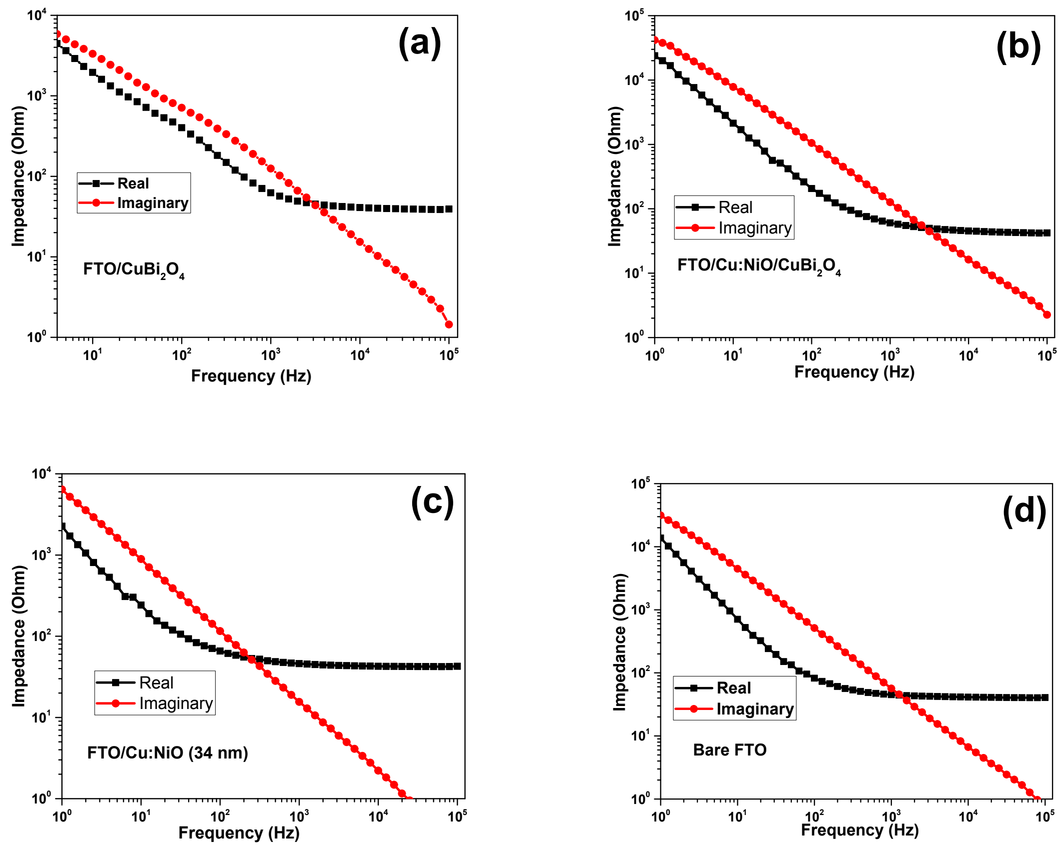

Figure S17. Electrochemical impedance spectroscopy (EIS) at 1.00 V vs. RHE for (a) $CuBi_2O_4$ deposited on FTO, (b) $CuBi_2O_4$ (260 nm) deposited on Cu:NiO (7 nm) on FTO, (c) Cu:NiO (34 nm) deposited on FTO, and (d) bare a FTO substrate. The measurements were performed in 0.3 M K_2SO_4 and 0.2 M phosphate buffer (pH 6.65). Note that above 1 kHz, the real part of the impedance is constant, whereas the imaginary part has a slope of -1. This implies that the system behaves as a resistance in series with a pure capacitance, which is a prerequisite for Mott-Schottky analysis.

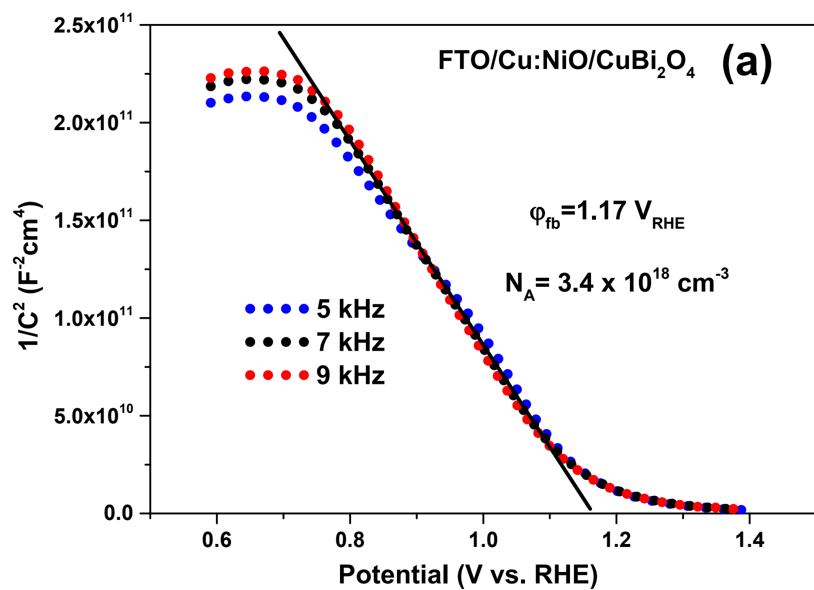
FTO/Cu:NiO/CuBi2O4
(a)
φfb=1.17 VRHE
NA= 3.4 x 10^18 cm^-3
5 kHz
7 kHz
9 kHz
1/C2 (F-2cm4)
Potential (V vs. RHE)

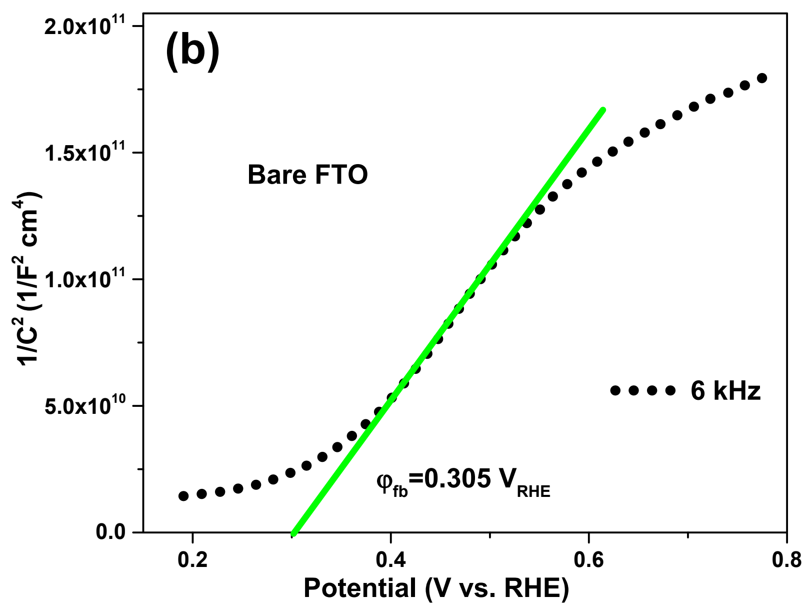
(b)
Bare FTO
6 kHz
φfb=0.305 VRHE
1/C2 (1/F2 cm4)
Potential (V vs. RHE)

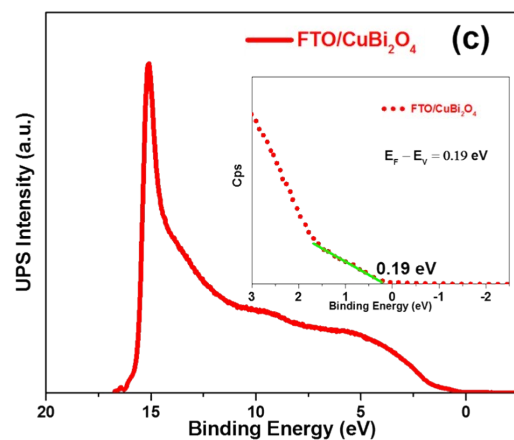

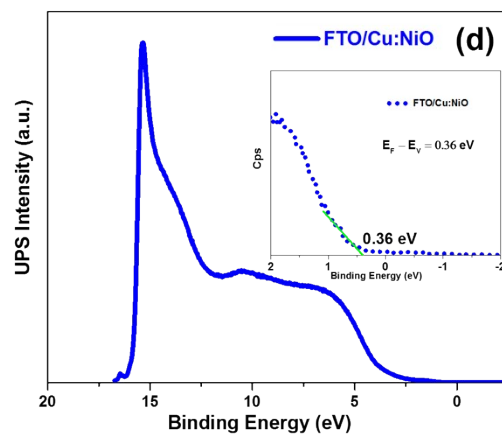

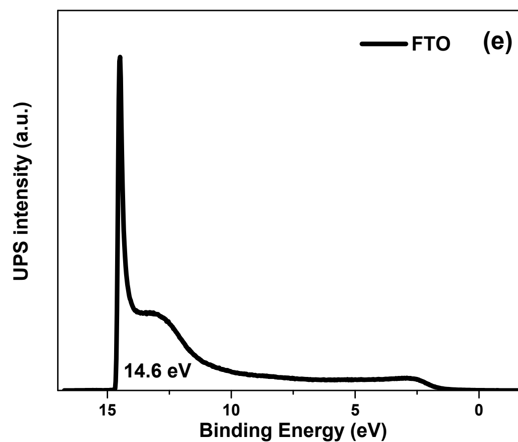

Figure S18. Mott−Schottky plots obtained for $CuBi_2O_4$ films and bare FTO. (a) Mott−Schottky of $CuBi_2O_4$ films deposited on 7 nm Cu:NiO film (b) Mott−Schottky of bare FTO. UPS cutoff spectra measured without bias for (c) $CuBi_2O_4$ and (d) Cu:NiO thickness of 34 nm deposited on FTO substrates and UPS cutoff spectra measured with a 2 V bias for a bare FTO substrate. Mott−Schottky measurements were performed in 0.3 M K_2SO_4 and 0.2 M phosphate buffer (pH 6.65) at 5 kHz, 7 kHz, and 9 kHz.

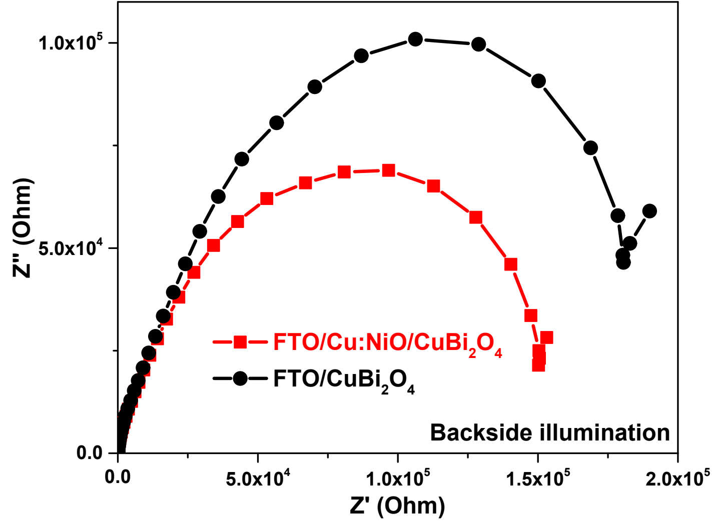

Figure S19. Electrochemical impedance spectroscopy (EIS) performed under backside illumination at 1.1 V vs. RHE for $CuBi_2O_4$ films deposited on FTO (black circle line) and 7 nm Cu:NiO layer (red square line).

Table S1. Summarizing Energy Levels

Material	Band Gap, E_g (eV)	Flat-Band Potential, φ_{fb} (eV / V vs. RHE)	Work Function, WF (eV / V vs. RHE)	Average, E_F (φ_{fb} & WF) (eV / V vs. RHE)	n-type N_A p-type N_D (cm^{-3})	p-type $\vert E_V - E_F \vert$ (eV)	Valence Band Offset $\vert E_V - E_F \vert$
FTO	3.7	4.81 / 0.31	4.61 / 0.11	4.71 / 0.21	1×10^{21}		
Cu:NiO	3.75	5.21 / 0.71	5.11 / 0.61	5.16 / 0.66	4.6×10^{18}	< 0.077	0.36
$CuBi_2O_4$	1.6	5.62 / 1.12	5.79 / 1.29	5.71 / 1.21	3.2×10^{18}	< 0.077	0.19

Table S2. Sheet resistance of different thickness of Cu:NiO thin films deposited on glass substrates.

As Deposited Thickness (nm)	Post Anneal Thickness (nm)	Film Sheet Resistance (Ω/□)	Film Resistivity (Ω m)
4.4	7	1.16×10^8	0.815
12	34	9.58×10^7	3.258
66	102	8.33×10^7	8.492

.